World Electric Vehicle Journal

MDPI

Article

Analysis of Efficiency and Noise, Vibration, and Hardness Characteristics of Inverter for Electric Vehicles According to Pulse Width Modulation Technique

Do-Yun Kim

Department of Smart Mobility, Pyeongtaek University, Room 215, Science & Engineering Building, 3825 Seodong-Daero, Pyeongtaek-si 17869, Gyeonggi-do, Republic of Korea; kimdoyun@ptu.ac.kr

Abstract: This study investigates the efficiency and noise, vibration, and harshness (NVH) characteristics of electric vehicle (EV) powertrains based on three key Pulse Width Modulation (PWM) techniques: Space Vector PWM (SVPWM), Discontinuous PWM (DPWM), and Random PWM (RPWM). The objective is to evaluate the impact of these PWM techniques on inverter and motor efficiency, as well as their effects on NVH performance, particularly in relation to noise and vibration. Experiments were conducted across various speed and torque levels using a motor dynamo. The study reveals that DPWM provides the highest efficiency, outperforming SVPWM by up to 2.23%. However, DPWM introduces more noise due to increased total harmonic distortion (THD), negatively affecting NVH performance. SVPWM, on the other hand, offers a balanced trade-off between efficiency and NVH, while RPWM demonstrates comparable noise characteristics to SVPWM, with potential for broader harmonic distribution. The findings suggest that each PWM technique offers distinct advantages, and their selection should depend on the required balance between efficiency and NVH.

Keywords: electric vehicles; torque control; efficiency optimization; harmonic analysis; motor drives

Citation: Kim, D.-Y. Analysis of Efficiency and Noise, Vibration, and Hardness Characteristics of Inverter for Electric Vehicles According to Pulse Width Modulation Technique. *World Electr. Veh. J.* **2024**, *15*, 546. https://doi.org/10.3390/wevj15120546

Academic Editors: Xinmin Li and Liyan Guo

Received: 22 October 2024
Revised: 20 November 2024
Accepted: 22 November 2024
Published: 23 November 2024

1. Introduction

The automobile industry is making various efforts to reduce greenhouse gas emissions and reduce dependence on fossil fuels by switching to electric vehicles (EVs) [1]. EVs do not directly use fossil fuels, so they reduce greenhouse gases, have high energy efficiency, etc. However, for smooth adoption of EVs, noise, vibration, and harshness (NVH) performance optimization is required for higher efficiency and comfortable driving for drivers [2,3].

The efficiency of an inverter, which converts DC power into the AC power required to drive an electric vehicle, is essential for overall powertrain performance. Various PWM techniques are key factors in determining this efficiency. These techniques play a crucial role not only in the efficiency of power conversion but also in the NVH (Noise, Vibration, and Harshness) characteristics of the system, directly affecting the driver's experience [4,5].

This paper investigates the effects of three Pulse Width Modulation (PWM) techniques—Space Vector PWM (SVPWM), Discontinuous PWM (DPWM), and Random PWM (RPWM)—on the efficiency and NVH characteristics of electric vehicle powertrains. These techniques are widely applied in EV driving systems due to their distinct advantages [6,7]. Through experimental analysis, we quantify the impact of each PWM method on motor efficiency and acoustic performance. SVPWM is shown to improve motor efficiency by up to 15% compared to traditional sinusoidal PWM [8]. DPWM techniques can further reduce switching losses, potentially increasing inverter efficiency by 20–30% [9]. RPWM, while less efficient, demonstrates superior NVH performance by spreading harmonic energy across a wider frequency spectrum, reducing the perception of tonal noise [10]. By elucidating the trade-offs between efficiency and NVH for each technique, this study provides crucial

insights for EV powertrain designers aiming to optimize both performance and driving comfort.

The main purpose of this study was to evaluate and compare the efficiency of inverters, motors, and inverter and motor integrated systems according to various PWM techniques, and to analyze the impact of these PWM techniques on NVH, especially focusing on noise. Through this, it is expected that a PWM technique can be selected to achieve the optimal balance between efficiency and NVH.

The structure of this paper is as follows. Section 2 introduces existing research on EV PWM technology, inverter performance, and NVH. Section 3 presents the method used in the experiment and presents the experimental results. Section 4 discusses the implications of these findings and concludes the paper with key analyses and suggestions for future research.

2. Literature Review of EV Inverter

2.1. Overview of Electric Vehicle (EV) Inverters

Voltage source inverters are commonly used in electric vehicles to convert DC power from the battery into AC power required for motor operation, as illustrated in Figure 1. The inverter consists of six switches, arranged in three arms, each responsible for producing one phase of the three-phase current. Each arm has a top and bottom switch that perform complementary switching operations to avoid short circuits in the arms [11,12].

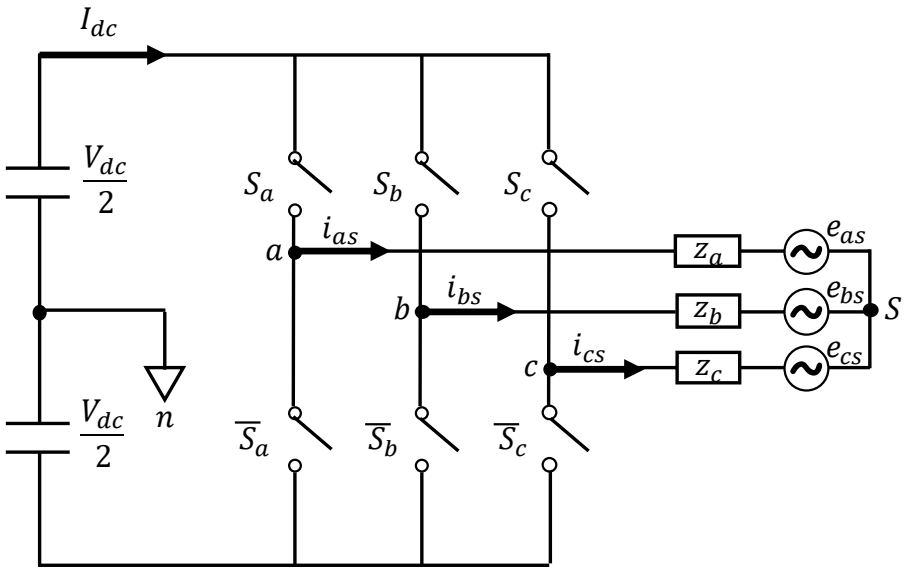

Figure 1. Three-phase inverter.

Typically, the continuous SVPWM technique is used to generate three-phase voltages efficiently. To further optimize performance, the DPWM technique can be applied to reduce switching losses, while the RPWM technique is often employed to mitigate NVH. Each of these techniques plays a key role in improving the inverter's efficiency and overall driving comfort.

2.2. Pulse Width Modulation Techniques

2.2.1. Space Vector PWM

One of the key performance indicators of PWM techniques is the magnitude of the output voltage produced when converting a limited direct current (DC) voltage into an alternating current (AC). Table 1 presents a comparison of the output voltages for different PWM techniques. Among these, the 6-Step technique can achieve the highest voltage. However, this technique operates by generating output voltages at intervals of 60 degrees in the frequency domain, producing six distinct voltage steps over 360 degrees. Due to its

discontinuous nature, the 6-Step technique is typically not used under normal operating conditions [13,14].

Table 1. Comparison of output voltage sizes according to PWM technique.

No	PWM Method	Output Voltage	P.U	Voltage Ratio
1	SPWM	$\frac{V_{dc}}{2}$	0.5	100 [%]
2	SVPWM	$\frac{V_{dc}}{\sqrt{3}}$	0.5773	115.47 [%]
3	6-Step	$\frac{2}{\pi}V_{dc}$	0.6366	127.324 [%]

Among continuous PWM techniques, SVPWM is capable of generating the highest output voltage. When compared to SPWM, which uses the same DC voltage input, SVPWM produces an output voltage that is 15.47% higher, making it a more efficient choice for generating alternating voltages in electric vehicle inverters.

The phase voltages V_{as}, V_{bs}, V_{cs}, and V_{cs} generated by the inverter can be expressed in terms of the switching functions S_a, S_b, and S_c, as shown in Figure 1. These switching functions determine the ON/OFF states of the inverter's switches, and the resulting phase voltages are described by Equation (1):

$$\begin{aligned} V_{as} &= \tfrac{V_{dc}}{3}(2S_a - S_b - S_c) \\ V_{bs} &= \tfrac{V_{dc}}{3}(2S_b - S_c - S_a) \\ V_{cs} &= \tfrac{V_{dc}}{3}(2S_c - S_a - S_b) \end{aligned} \quad (1)$$

The switching function controls the output voltages for each phase. Depending on the combination of switching states, a total of eight possible voltage vectors can be generated by the inverter. These eight vectors are represented graphically as a space vector in Figure 2.

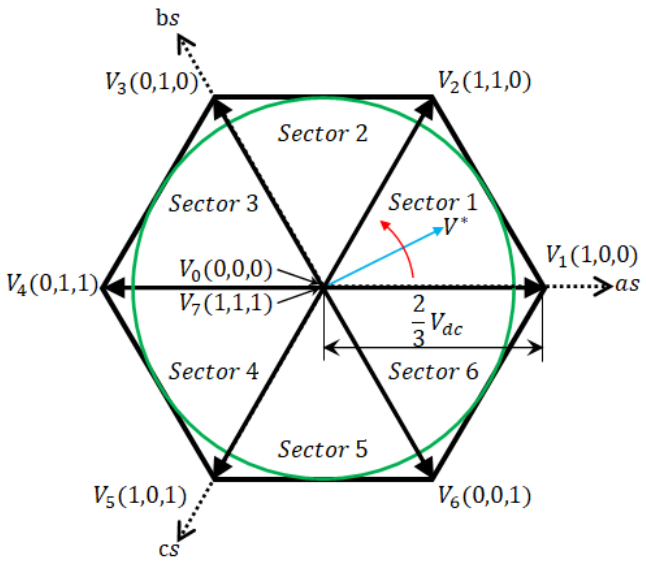

Figure 2. Space vector method.

The change in the inverter's three-phase switching command causes the command voltage vector V^* to rotate counterclockwise in the space vector plane (d-q axis stationary coordinate plane), as illustrated in Figure 2. During each cycle of the command voltage, the voltage vector completes one full rotation.

SVPWM generates the desired command voltage by using the eight available switching vectors. Specifically, two adjacent effective voltage vectors, V_n and V_{n+1}, which are closest to the command voltage vector V^*, are selected. In addition, zero-voltage vectors V_0 and V_7 are used to maintain the average output voltage during each modulation period T_s.

The time allocated to apply each vector is as follows: T_1 for the first vector V_n, T_2 for the second vector V_{n+1}, and T_0 for the zero vectors. The composition of the voltage using the vectors V_n and V_{n+1} and the zero vectors during T_s is described by Equation (2):

$$\begin{gathered}\int_0^{T_s} V^* dt = \int_0^{T_1} V_n dt + \int_{T_1}^{T_1+T_2} V_{n+1} dt + \int_{T_1+T_2}^{T_s} V_{0,7} dt, \\ (\therefore V^* T_s = V_n T_1 + V_{n+1} T_2).\end{gathered} \tag{2}$$

Among the various Space Vector Pulse Width Modulation (SVPWM) techniques that combine two adjacent effective voltage vectors with zero-voltage vectors, the symmetrical space vector voltage modulation method stands out for its efficiency and balanced performance. This method involves placing the effective vector application time $T_1 + T_2$ exactly at the center of one cycle of voltage modulation T_s, thereby achieving symmetry within the modulation cycle. As a result, the effective voltage vector is positioned at the center, while the zero vectors are located at the beginning and end of the cycle. This symmetrical arrangement ensures that the ripple of the phase current within each cycle maintains a symmetrical shape, thereby reducing the number of switching events required [15,16].

Figure 3 illustrates the switching status in the sector 1 area, providing a visual representation of how the symmetrical SVPWM operates. In this figure, the top switch of phase A remains ON while the bottom switch stays OFF, and phases B and C perform complementary switching operations [17]. This coordinated switching pattern is fundamental to maintaining the symmetry and minimizing harmonic distortions in the output voltage. By ensuring that all three-phase switches undergo switching operations within each modulation cycle, symmetric SVPWM is classified as a continuous modulation method. This continuous approach not only enhances voltage utilization but also contributes to smoother motor operation and reduced electromagnetic interference (EMI).

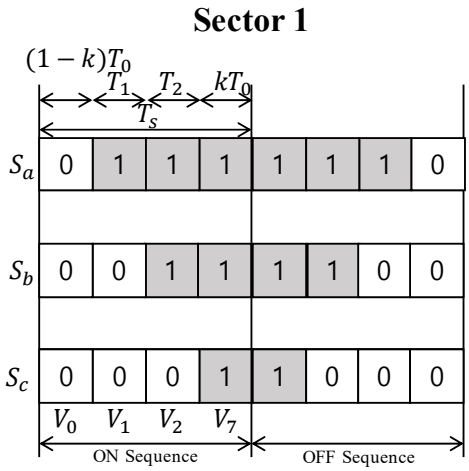

Figure 3. Switching status in sector 1 of SVPWM.

Symmetric SVPWM is the most widely used SVPWM technique due to its ability to balance efficiency and NVH performance. By maintaining continuous switching across all phases and achieving a symmetrical current ripple, this method optimizes the inverter's performance, making it highly suitable for electric vehicle applications where both efficiency and driving comfort are paramount.

2.2.2. Discontinuous PWM

Unlike the continuous voltage modulation method, DPWM is a technique designed to reduce the number of switching events by switching only two of the three inverter phases. The main goal of applying DPWM is to increase the efficiency of the inverter by reducing switching losses. However, the harmonic characteristics vary depending on the placement of the non-switching discontinuous section.

In the discontinuous modulation method, the symmetry of the effective voltage vector is lost, but the number of switching operations is reduced to two-thirds of the continuous modulation method. When the discontinuous section is inserted at an optimal position—especially in areas with a high voltage modulation index—it can result in better harmonic performance than continuous modulation methods, even when operating at the same switching frequency. In regions with a low modulation index, however, the loss of symmetry in the effective voltage vector can lead to an increase in harmonic distortion compared to continuous modulation techniques [18–20].

Reflecting on these characteristics, research has been conducted into various discontinuous section placements, resulting in six distinct DPWM techniques: 60°, 60° + 30°, 60° − 30°, 30°, +120°, and −120° DPWM. Each technique has different harmonic characteristics based on the placement of the non-switching phase.

Figure 4 shows the switching status of DPWM in sector 1. In this example, the top switch of phase A remains ON, the bottom switch remains OFF, and phases B and C perform the necessary switching operations.

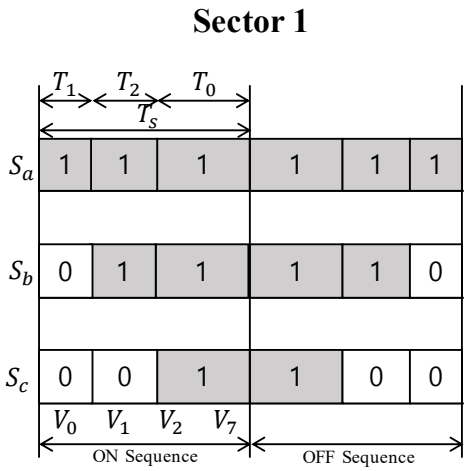

Figure 4. Switching status in sector 1 of DPWM.

The three-phase inverter can be configured with a 120° discontinuous modulation section, during which no switching occurs in one phase over a cycle of the command voltage. Although the discontinuous section can be placed at any position within the command voltage cycle, it is generally positioned near the maximum phase current. This is because switching losses are proportional to the amount of current flowing through the switch, and placing the discontinuous section at the point of maximum current helps to reduce switching losses.

To achieve optimal efficiency, the placement of the discontinuous section must be adjusted based on the load status. Under different load conditions, the discontinuous section may need to be rearranged to further reduce losses and maintain performance.

In the 60° discontinuous modulation method, switching is not performed during the 60° section of the modulation cycle where the phase voltage reaches its maximum or minimum value. This approach is especially useful for applications like UPS systems, grid-connected inverters, and permanent magnet synchronous motor drives, where the voltage and current are controlled to be nearly in phase. By eliminating switching in these sections, switching losses can be minimized.

Figure 5a provides an example of the a-phase pole voltage command used to implement this modulation method. During the 60° section where the phase static voltage command V_{as}^{*} is at its most positive, the upper switch of phase A remains on, and the pole voltage command V_{an}^{*} is set to $V_{dc}/2$. Conversely, during the most negative 60° section, the lower switch is kept on by fixing the pole voltage command at $-V_{dc}/2$.

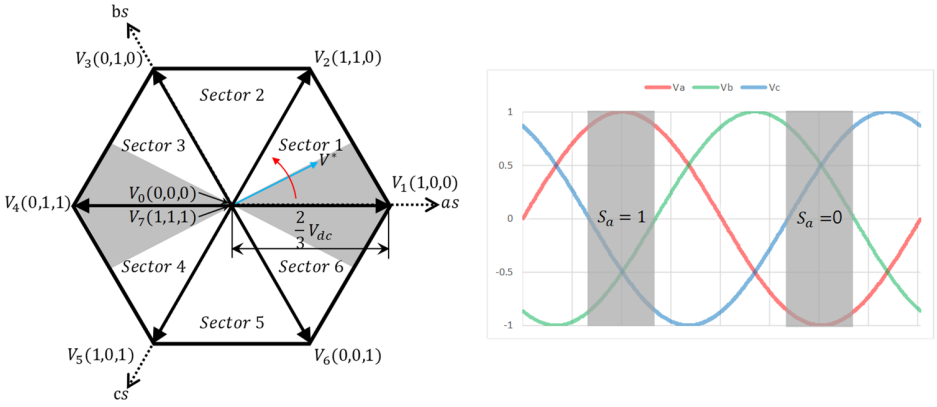

(**a**) 60° DPWM

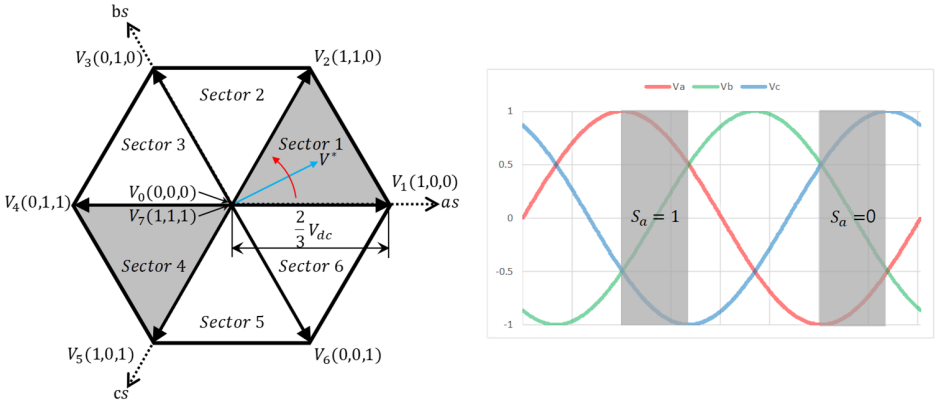

(**b**) 60° +30° DPWM

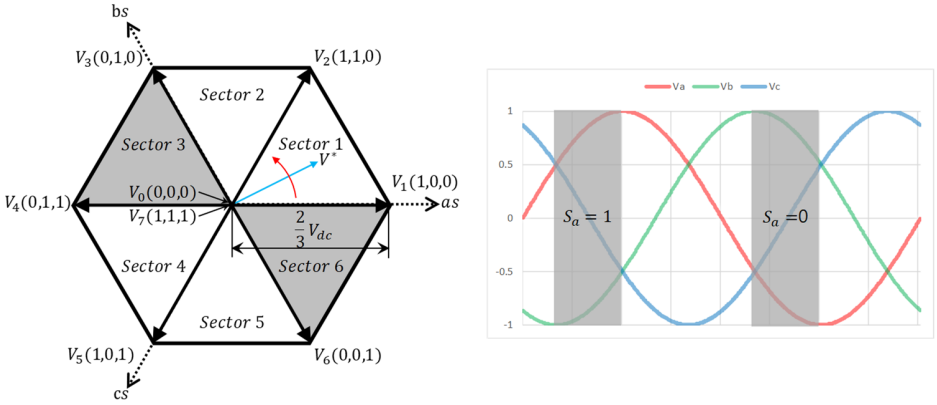

(**c**) 60° −30° DPWM

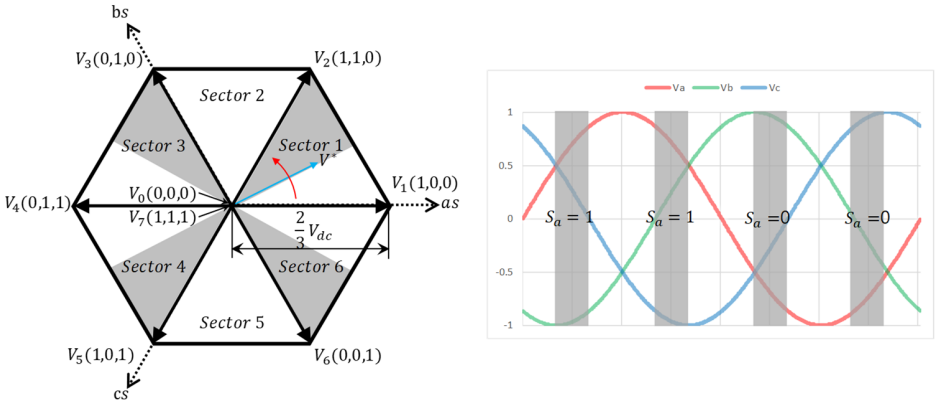

(**d**) 30° DPWM

Figure 5. *Cont.*

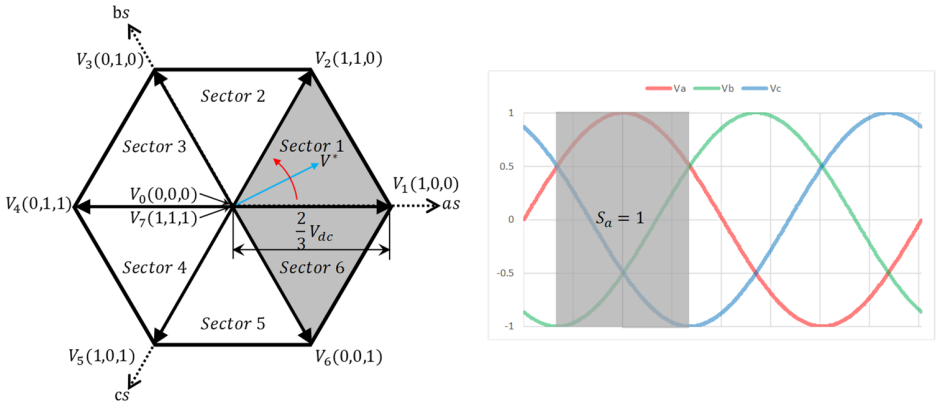

(**e**) +120° DPWM

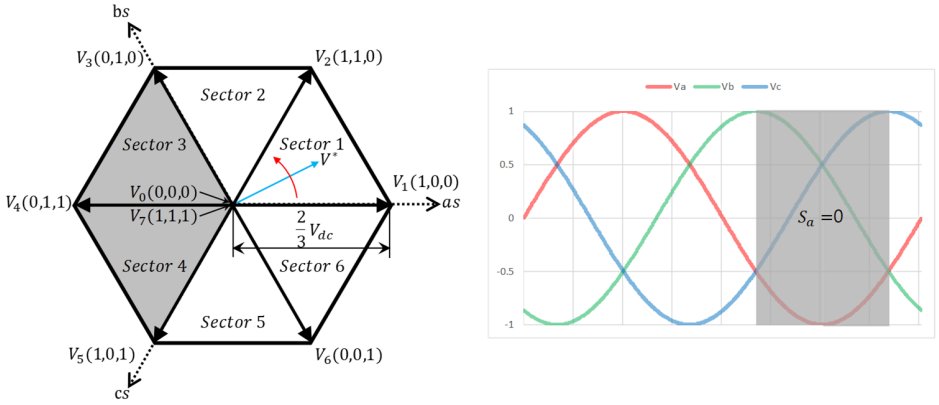

(**f**) −120° DPWM

Figure 5. Switching patterns of a-phase with six types of DPWM applied.

In the case of an R+XL load, such as an induction motor, the current lags behind the input voltage. This lagging current is a typical characteristic of inductive loads. The main goal of using the discontinuous modulation method is to reduce switching losses when the current reaches its maximum value.

To address the current flowing to the ground in relation to the phase voltage, a 60° + 30° discontinuous modulation method is applied. In this technique, switching is avoided during the 30° delayed section, resulting in discontinuous modulation within the 60° to 120° portion of the cycle. This helps to minimize switching losses, especially when dealing with a lagging current.

Figure 5b illustrates the space vector diagram for the 60° + 30° discontinuous modulation method, along with the sectors where discontinuous modulation is applied.

The 30° discontinuous modulation method is widely regarded as the best approach for reducing harmonic losses. In this technique, the discontinuous modulation area added to one complete cycle covers a total of 120°. However, in the 30° discontinuous modulation method, this area is distributed across four specific regions.

The four areas where discontinuous modulation is performed are as follows:

30° to 60°, 120° to 150°, 210° to 240°, and 300° to 330°.

This division allows for optimized performance in minimizing harmonic distortions. Figure 5d illustrates the space vector diagram for this modulation method, showing the sectors where discontinuous modulation occurs.

The 120° discontinuous modulation method is a technique where switching is avoided for one-third of a cycle (120°). This method is suitable for low-cost systems due to its ability to reduce switching frequency and complexity.

However, there are some drawbacks. The +120° and −120° discontinuous modulation methods result in uneven switching losses between the upper and lower switches of the inverter. While the +120° method effectively reduces the switching losses in the lower

switch, and the −120° method focuses on the upper switch, this imbalance can be a disadvantage. Although the overall switching losses are reduced, this method does not offer any significant improvement in the inverter's maximum output performance.

Figure 5e illustrates the space vector diagram for the +120° discontinuous modulation method and highlights the sectors where discontinuous modulation occurs.

Figure 5f shows the space vector diagram for the −120° discontinuous modulation method and highlights the sectors where discontinuous modulation is applied.

2.2.3. Random PWM

When controlling an inverter using the PWM technique, harmonics tend to concentrate in the output voltage within specific frequency bands, particularly those corresponding to the switching frequency and its multiples, as well as the associated sidebands. These harmonics can lead to undesirable effects such as noise and vibration. To mitigate these issues, RPWM has emerged as a promising technique that reduces the impact of harmonics without increasing the overall switching frequency [21].

RPWM operates by introducing random variables to alter the inverter's switching pattern, effectively dispersing the harmonic spectrum across a broader frequency range. This is significant because the ripple in the phase current typically exhibits peaks at frequencies tied to the inverter's switching frequency, the output voltage frequency, and the natural characteristics of the load. Such specific frequency ripples can induce vibrations and noise in connected loads [22,23].

Moreover, with the rising concern over EMI due to power converters, RPWM offers a valuable solution by spreading high-frequency components—often concentrated around the switching frequency and its harmonics—across a wider frequency band. This results in a more symmetrical current profile, minimizing potential EMI issues.

In this paper, we have implemented a Random PWM technique that maintains a constant switching frequency while utilizing offset voltage modulation. This approach is particularly advantageous as it simplifies implementation; it involves merely adding a randomization function to the offset voltage, based on the previously established offset voltage modulation with SVPWM. Importantly, this can be achieved without the need for additional hardware or complex algorithms, making it an efficient choice for practical applications.

The voltage modulation method utilizing offset voltage is an integrated approach that facilitates the easy implementation of various existing voltage modulation techniques. As depicted in Figure 6, this method integrates Random RPWM by incorporating a random function into the pole voltage calculated for SVPWM in the context of SVPWM.

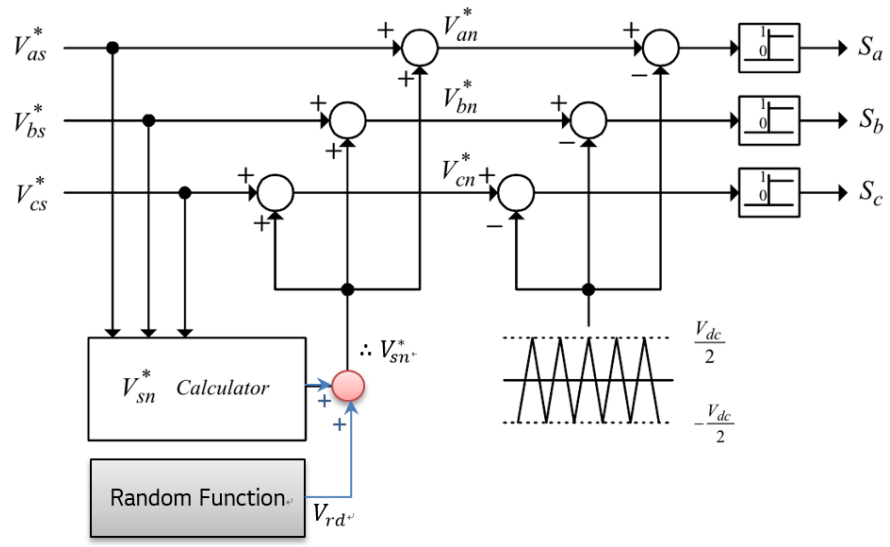

Figure 6. RPWM algorithm block diagram with offset voltage technique applied.

The offset voltage (V_{sn}^*) generated through this randomization process is represented mathematically in Equation (3), showcasing how the random function influences the overall voltage modulation. V_{sn}^* is calculated as follows:

$$V_{sn}'' = -\frac{V_{max}^* + V_{min}^*}{2} + V_{rd} \tag{3}$$

2.3. Contemplation of Harmonics in General PWM Techniques

The primary objective of the PWM technique is to control the switches in each phase to generate a fundamental wave voltage with the same magnitude and frequency as the command voltage. Various PWM techniques have been developed, starting with sinusoidal PWM (SPWM). The performance of a PWM technique is evaluated based on its ability to linearly output the voltage within the constraints of the DC link voltage and the harmonic characteristics of the output voltage. The voltage modulation index (MI), defined in Equation (4),

$$V_{p-h} = V_h sin\Big(Mm_f \pm N\Big)[2\pi f_0 t + \varnothing_h], \tag{4}$$

is used to describe the output voltage magnitude for each phase in PWM techniques.

Compared to SPWM, SVPWM has a voltage modulation index approximately 1.155 times higher, meaning it utilizes the DC link voltage more effectively. However, the output voltage of the inverter contains harmonics concentrated around specific frequencies—specifically the switching frequency f_c, its multiples M, and the sidebands at Nf_0.

Equation (4) represents the harmonic components of the pole voltage V_p caused by PWM switching, where f_0 is the fundamental frequency of the output voltage, and m_f is the frequency modulation index, which is the ratio of the switching frequency to the fundamental frequency, as defined in Equation (5):

$$m_f = \frac{f_c}{f_0} \tag{5}$$

Here, M and N are integers, and their sum $(M + N)$ must be odd. The harmonic orders from Equation (4) are as follows:

$$\begin{array}{cccccc} m_f & m_f \pm 2 & m_f \pm 4 & m_f \pm 6 & \dots \\ 2m_f + 1 & 2m_f \pm 3 & 2m_f \pm 5 & 2m_f \pm 7 & \dots \\ 3m_f & 3m_f \pm 2 & 3m_f \pm 4 & 3m_f \pm 6 & \dots \end{array} \tag{6}$$

Among these harmonic components, those of order m_f are the largest. In other words, the harmonic components associated with the switching frequency f_c are the most dominant. Figure 7 illustrates the harmonic distribution of pole voltages for general PWM techniques.

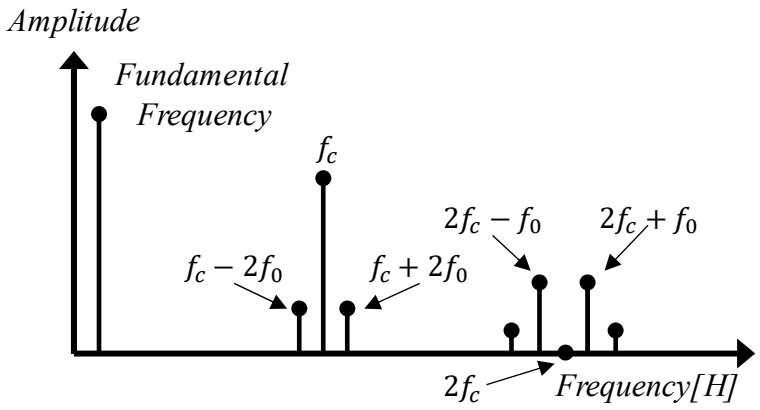

Figure 7. Harmonic distribution of pole voltages in common PWM techniques.

The harmonic characteristics for the line voltage and phase voltage are further detailed in Figure 8. In a three-phase inverter driving system, harmonic components that are multiples of three are effectively removed from the line-to-line voltage calculated as the difference between pole voltages. Since these components are in phase within each phase voltage, they do not contribute to the line voltage.

If the frequency modulation index m_f is set to a multiple of three, all harmonics that are multiples of m_f can be eliminated from the line voltage, leading to a reduction in the overall harmonic content. Consequently, the largest harmonic component m_f is also removed, resulting in the following harmonic components:

$$\begin{array}{cccc} \cancel{m_f} & m_f \pm 2 & m_f \pm 4 & m_f \pm 6 & \ldots \\ 2m_f + 1 & \cancel{2m_f \pm 3} & 2m_f \pm 5 & 2m_f \pm 7 & \ldots \\ \cancel{3m_f} & \cancel{3m_f \pm 2} & 3m_f \pm 4 & 3m_f \pm 6 & \ldots \end{array} \tag{7}$$

Figure 8 illustrates the harmonic distribution of the line voltage when m_f is a multiple of three. These harmonics, concentrated in specific frequency bands, contribute to noise, vibration, and electromagnetic interference issues.

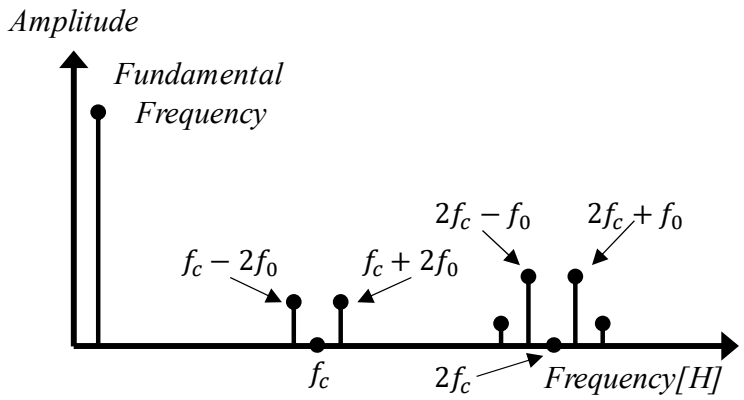

Figure 8. Harmonic distribution of line voltage in common PWM techniques.

As a method to evaluate the harmonic-spectrum spread effect of the random PWM technique, the harmonic spread factor (HSF), a concept derived from standard deviation in probability theory, can be applied. The HSF is calculated using the following formula:

$$HSF = \sqrt{\frac{1}{N-1}\sum_{j>1}^{N}\left(H_j - H_0\right)^2} \tag{8}$$

In these equations, H_j refers to the magnitude of the j-th individual harmonic, and H_0 represents the average of $N-1$ harmonics. An ideal harmonic diffusion effect is achieved when the HSF equals 0, which corresponds to the condition of ideal white noise. The equation for H_0 can be expressed as follows:

$$H_0 = \frac{\sum_{j>1}^{N} H_j}{N-1} \tag{9}$$

Additionally, an analysis of total harmonic distortion (THD) is necessary to examine the impact of harmonic characteristics when applying the Random PWM technique. THD is expressed by the following equation:

$$THD = \frac{\sqrt{\sum_{j>1}^{N} V_j^2}}{V_1} \tag{10}$$

where V_1 is the root mean square (rms) value of the output voltage fundamental wave, and V_j represents the rms value of the j-th harmonic. This analysis provides insight into how effectively the Random PWM technique can minimize harmonic distortions while maximizing efficiency.

3. Experimental Results

3.1. Efficiency Measurements

The efficiency test was conducted using a motor dynamo, with power measurements taken by Yokogawa's WT3000 power meter. The experimental procedure first presents the inverter's efficiency by analyzing its performance based on varying speed and torque values. Following this, the motor efficiency is evaluated under similar conditions. Finally, the combined efficiency of the inverter and motor system is presented, showcasing how the entire system performs across different operational ranges. This stepwise approach allows for a detailed comparison of each component's efficiency and their integrated performance. Figure 9 illustrates the command voltage patterns for SVPWM, DPWM, and RPWM techniques, highlighting their distinct characteristics. In SVPWM, the command voltage is represented by a rotating voltage vector that covers the full 360-degree space, aiming for continuous modulation to maximize voltage utilization while maintaining balanced switching across all three phases.

DPWM, on the other hand, introduces non-switching periods in the command voltage, where only two out of the three phases are actively switching, effectively reducing switching losses. This results in distinct discontinuous sections in the command voltage. Lastly, RPWM incorporates random variations in the switching pattern of the command voltage, dispersing harmonics across a wider frequency spectrum. This technique aims to reduce the concentration of harmonics in specific frequency bands, thereby improving NVH and reducing EMI. Figure 9 visually captures these differences in the modulation behavior of each technique.

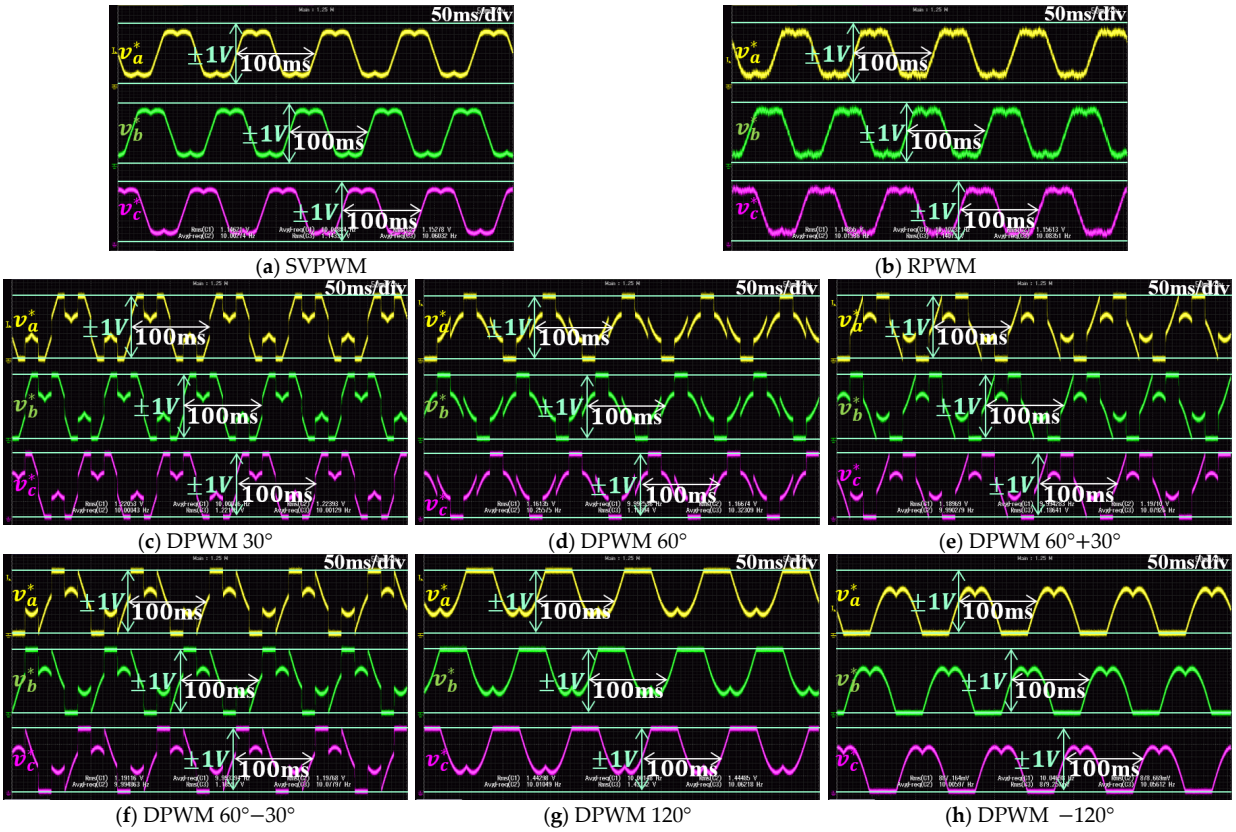

(**a**) SVPWM (**b**) RPWM

(**c**) DPWM 30° (**d**) DPWM 60° (**e**) DPWM 60°+30°

(**f**) DPWM 60°−30° (**g**) DPWM 120° (**h**) DPWM −120°

Figure 9. Three-phase voltage commands of SVPWM, RPWM, and DPWM.

The experimental conditions are shown in Table 2.

Table 2. Experimental conditions.

Parameters	Value	Unit
DC Voltage	400	V
Speed range	1000~10,000	rpm
Torque range	20~300	Nm
Pole pair	4	-
$L_d/L_q/R_s$	0.168/0.632/0.0135	mH/mH/Ω

3.1.1. Inverter Efficiency Results

In Figure 10, the inverter efficiency results according to the PWM technique are presented based on speed and torque. Figure 10a shows the efficiency (%) obtained when applying the SVPWM technique. In contrast, Figure 10b displays the efficiency (%) results of the highest performing PWM technique chosen from the DPWM and RPWM methods. Figure 10c provides a comparative analysis of the techniques, where number 1 represents SVPWM, numbers 2 to 7 represent different DPWM methods, and number 8 corresponds to RPWM. The results indicate that the PWM technique has the highest efficiency based on speed and torque measurements. Finally, Figure 10d highlights the efficiency difference between the PWM technique selected in Figure 10b and the baseline SVPWM in Figure 10a. As demonstrated by these test results, the inverter's efficiency is highest when applying the DPWM technique, showing an improvement ranging from a minimum of 0.35% to a maximum of 2.23% compared to SVPWM.

Torque(Nm) / %

Torque(Nm)	1,000	2,000	3,000	4,000	5,000	6,000	7,000	8,000	9,000	10,000
300	89.62	93.73	95.45							
280	89.86	94.17	95.72							
260	90.15	94.49	95.96							
240	90.49	94.75	96.20	96.62						
220	90.62	94.85	96.29	96.76						
200	90.81	94.97	96.45	96.98	96.81					
180	90.94	95.05	96.57	97.14	97.01					
160	90.96	95.07	96.58	97.17	97.05	96.91				
140	91.00	95.13	96.60	97.27	97.16	97.04	96.89			
120	91.03	95.17	96.62	97.34	97.23	97.13	96.95	97.01		
100	91.05	95.19	96.63	97.37	97.27	97.17	96.98	97.01		
80	90.84	95.09	96.56	97.35	97.26	97.08	96.85	96.89	96.97	97.20
60	90.59	94.98	96.48	97.32	97.24	96.98	96.70	96.76	96.79	96.94
40	90.34	94.87	96.39	97.29	97.22	96.87	96.54	96.62	96.60	96.68
20	90.65	94.71	96.28	97.17	96.90	96.85	96.44	96.50	96.46	96.58

Speed(rpm)

(**a**) Efficiency test results applying SVPWM.

Torque(Nm) / %

Torque(Nm)	1,000	2,000	3,000	4,000	5,000	6,000	7,000	8,000	9,000	10,000
300	91.76	94.92	96.60							
280	92.20	95.41	96.63							
260	92.46	95.69	96.86							
240	92.76	95.92	97.07	97.33						
220	92.88	96.01	97.15	97.45						
200	93.06	96.17	97.30	97.64	97.46					
180	93.19	96.29	97.40	97.77	97.63					
160	93.22	96.31	97.42	97.80	97.67	97.51				
140	93.30	96.38	97.47	97.90	97.79	97.64	97.42			
120	93.35	96.43	97.50	97.97	97.88	97.73	97.54	97.50		
100	93.38	96.45	97.52	98.00	97.92	97.77	97.59	97.55		
80	93.31	96.41	97.51	98.01	97.92	97.73	97.51	97.48	97.45	97.55
60	93.22	96.37	97.49	98.03	97.92	97.68	97.41	97.40	97.37	97.42
40	93.13	96.32	97.47	98.04	97.91	97.62	97.31	97.31	97.28	97.28
20	93.56	95.98	97.31	97.67	97.72	97.57	96.82	96.85	96.80	97.08

Speed(rpm)

(**b**) Efficiency test results applying DPWM and RPWM.

Torque(Nm)

Torque(Nm)	1,000	2,000	3,000	4,000	5,000	6,000	7,000	8,000	9,000	10,000
300	4	4	4							
280	4	4	4							
260	4	4	4							
240	4	4	4	4						
220	4	4	4	4						
200	4	4	4	4	4					
180	4	4	4	4	4					
160	3	4	4	1	3	4				
140	3	4	4	1	3	1	4			
120	3	4	3	2	3	2	3	4		
100	3	4	3	3	3	3	3	3		
80	4	3	3	3	5	5	5	5	3	3
60	4	3	3	3	5	5	5	5	3	3
40	4	3	3	3	5	5	5	5	5	5
20	4	3	3	3	5	5	5	5	5	5

SVPWM	1
30°DPWM	2
60°DPWM	3
60°+30°DPWM	4
60°-30°DPWM	5
+120°DPWM	6
-120°DPWM	7
RPWM	8

Speed(rpm)

(**c**) Results of selection of maximum-efficiency PWM.

Torque(Nm) / RDPWM-SWPWM(%)

Torque(Nm)	1,000	2,000	3,000	4,000	5,000	6,000	7,000	8,000	9,000	10,000
300	2.15	1.19	1.15							
280	2.34	1.24	0.91							
260	2.31	1.20	0.90							
240	2.27	1.17	0.87	0.71						
220	2.26	1.16	0.86	0.69						
200	2.25	1.20	0.85	0.66	0.65					
180	2.25	1.24	0.83	0.63	0.62					
160	2.26	1.24	0.84	0.63	0.62	0.60				
140	2.30	1.25	0.87	0.63	0.63	0.60	0.53			
120	2.32	1.26	0.88	0.63	0.65	0.60	0.59	0.49		
100	2.33	1.26	0.89	0.63	0.65	0.60	0.61	0.54		
80	2.47	1.32	0.95	0.66	0.66	0.65	0.66	0.59	0.48	0.35
60	2.63	1.38	1.02	0.71	0.67	0.70	0.72	0.64	0.58	0.47
40	2.79	1.45	1.08	0.75	0.69	0.75	0.77	0.69	0.68	0.60
20	2.92	1.27	1.03	0.50	0.82	0.72	0.38	0.36	0.34	0.50

Speed(rpm)

(**d**) Efficiency comparison results (D/RPWM−SVPWM).

Figure 10. Comparison of inverter efficiency measurement results by speed and torque with SVPWM, RPWM, and DPWM applied.

3.1.2. Motor Efficiency Results

In Figure 11, the motor efficiency results according to the PWM technique are analyzed based on speed and torque. Figure 11a illustrates the efficiency (%) when the SVPWM technique is applied. Figure 11b presents the efficiency (%) for the PWM technique that achieved the highest efficiency among the DPWM and RPWM techniques. In Figure 11c, the test results compare the best performing techniques, where number 1 represents SVPWM, numbers 2 through 7 represent various DPWM methods, and number 8 represents RPWM. Figure 11d highlights the efficiency difference between the PWM technique selected in Figure 11b and the baseline SVPWM in Figure 11a.

The results demonstrate that overall, the motor's efficiency is highest when using the SVPWM technique. Although RPWM and DPWM show higher efficiency in certain regions, the DPWM technique primarily reduces switching loss, but at the cost of increasing the THD of the output current. It is noted that the difference in efficiency between the various PWM techniques is less than 0.89%, indicating that the impact of switching technique on motor efficiency is minimal.

Torque(Nm) | %

Torque(Nm)	1,000	2,000	3,000	4,000	5,000	6,000	7,000	8,000	9,000	10,000
300	83.01	89.48	91.59							
280	83.20	89.59	92.05							
260	85.28	90.85	93.19							
240	87.52	91.98	93.97	94.15						
220	88.39	92.42	94.28	94.55						
200	89.76	93.19	94.74	95.10	94.00					
180	90.75	93.74	95.07	95.50	94.54					
160	91.02	93.85	95.13	95.57	94.66	93.69				
140	91.85	94.18	95.33	95.79	95.02	94.05	92.53			
120	92.44	94.41	95.47	95.95	95.28	94.30	93.02	92.04		
100	92.71	94.52	95.53	96.02	95.40	94.42	93.25	92.35		
80	93.03	94.48	95.40	95.74	95.22	94.21	93.06	92.14	90.97	90.28
60	93.41	94.44	95.25	95.42	95.01	93.96	92.85	91.90	90.58	90.18
40	93.79	94.40	95.10	95.10	94.79	93.71	92.63	91.65	90.18	90.07
20	93.96	94.38	94.98	94.99	94.37	93.55	92.61	91.35	89.92	89.70

Speed(rpm)

(**a**) Efficiency test results applying SVPWM.

Torque(Nm) | %

Torque(Nm)	1,000	2,000	3,000	4,000	5,000	6,000	7,000	8,000	9,000	10,000
300	83.10	89.51	92.09							
280	83.20	89.62	92.19							
260	85.55	90.93	93.19							
240	87.59	92.03	93.97	94.15						
220	88.39	92.46	94.28	94.55						
200	89.76	93.20	94.74	95.10	94.00					
180	90.75	93.74	95.07	95.50	94.58					
160	91.02	93.86	95.13	95.57	94.69	93.69				
140	91.85	94.22	95.33	95.79	95.04	94.08	92.54			
120	92.44	94.47	95.47	95.95	95.29	94.35	93.02	92.04		
100	92.71	94.59	95.53	96.02	95.40	94.48	93.25	92.35		
80	93.06	94.54	95.40	95.74	95.22	94.34	93.06	92.14	91.18	90.32
60	93.47	94.49	95.25	95.42	95.01	94.17	92.85	91.90	91.13	90.20
40	93.87	94.43	95.10	95.10	94.79	94.00	92.63	91.65	91.07	90.07
20	94.17	94.26	94.93	94.66	94.38	93.63	92.16	91.56	90.72	89.97

Speed(rpm)

(**b**) Efficiency test results applying DPWM and RPWM.

Torque(Nm)

Torque(Nm)	1,000	2,000	3,000	4,000	5,000	6,000	7,000	8,000	9,000	10,000
300	8	8	8							
280	1	8	8							
260	8	8	1							
240	1	8	1	1						
220	1	8	1	1						
200	1	1	1	1	1					
180	1	1	1	1	8					
160	1	8	1	1	1	1				
140	1	8	1	1	1	8	8			
120	1	8	1	1	1	8	1	1		
100	1	8	1	1	1	8	1	1		
80	8	8	1	1	1	6	1	1	2	4
60	8	8	1	1	1	6	1	1	2	4
40	8	8	1	1	1	6	1	1	8	1
20	8	8	1	1	1	6	1	1	8	1

SVPWM	1
30°DPWM	2
60°DPWM	3
60°+30°DPWM	4
60°-30°DPWM	5
+120°DPWM	6
-120°DPWM	7
RPWM	8

Speed(rpm)

(**c**) Results of selection of maximum-efficiency PWM.

Torque(Nm) | RDPWM-SWPWM(%)

Torque(Nm)	1,000	2,000	3,000	4,000	5,000	6,000	7,000	8,000	9,000	10,000
300	0.01	0.02	0.50							
280	0.00	0.03	0.14							
260	0.27	0.08	0.00	0.00						
240	0.07	0.05	0.00	0.00						
220	0.00	0.04	0.00	0.00	0.00					
200	0.00	0.01	0.00	0.00	0.00					
180	0.00	0.00	0.00	0.00	0.04	0.00				
160	0.00	0.01	0.00	0.00	0.03	0.00	0.01			
140	0.00	0.04	0.00	0.00	0.02	0.03	0.01	0.00		
120	0.00	0.06	0.00	0.00	0.01	0.05	0.00	0.00	0.00	
100	0.00	0.07	0.00	0.00	0.00	0.06	0.00	0.00	0.00	
80	0.03	0.06	0.00	0.00	0.00	0.13	0.00	0.00	0.21	0.04
60	0.06	0.05	0.00	0.00	0.00	0.21	0.00	0.00	0.55	0.02
40	0.08	0.03	0.00	0.00	0.00	0.29	0.00	0.00	0.89	0.00
20	0.11	0.07	0.00	0.00	0.00	0.29	0.00	0.00	0.80	0.00

Speed(rpm)

(**d**) Efficiency comparison results (D/RPWM−SVPWM).

Figure 11. Comparison of motor efficiency measurement results by speed and torque with SVPWM, RPWM, and DPWM applied.

3.1.3. Inverter and Motor Efficiency Results

Figure 12 presents the results of measuring the efficiency of the combined inverter and motor system based on different PWM techniques as a function of speed and torque. Figure 12a shows the system efficiency (%) when SVPWM is applied, while Figure 12b displays the experimental efficiency (%) for the PWM technique that achieved the highest efficiency among the DPWM and RPWM techniques. Figure 12c highlights the PWM technique with the highest efficiency, selected after comparing the results from SVPWM,

DPWM, and RPWM, where number 1 represents SVPWM, numbers 2 through 7 correspond to various DPWM techniques, and number 8 represents RPWM. Finally, Figure 12d compares the efficiency of the selected DPWM and RPWM techniques from Figure 12b with the baseline SVPWM.

The results indicate that the overall system efficiency is highest when the DPWM technique is applied. Although SVPWM and RPWM show competitive efficiency in some regions, the maximum efficiency difference between the PWM techniques is less than 2.13%. The DPWM technique consistently outperforms the others, demonstrating its effectiveness in reducing switching losses while maintaining high system efficiency.

Torque(Nm) | %

	1,000	2,000	3,000	4,000	5,000	6,000	7,000	8,000	9,000	10,000
300	74.42	83.88	87.89							
280	74.76	84.37	88.11							
260	76.88	85.84	89.43							
240	79.20	87.15	90.40	90.97						
220	80.10	87.66	90.78	91.49						
200	81.51	88.50	91.38	92.23	91.00					
180	82.53	89.10	91.81	92.77	91.71					
160	82.79	89.22	91.88	92.87	91.86	90.79				
140	83.58	89.59	92.09	93.18	92.32	91.26	89.65			
120	84.15	89.85	92.24	93.39	92.64	91.59	90.19	89.29		
100	84.41	89.97	92.31	93.49	92.80	91.75	90.43	89.59		
80	84.51	89.85	92.12	93.20	92.60	91.46	90.13	89.28	88.21	87.75
60	84.62	89.71	91.90	92.86	92.38	91.12	89.78	88.92	87.66	87.42
40	84.73	89.56	91.67	92.52	92.15	90.78	89.43	88.55	87.11	87.08
20	84.96	89.26	91.65	92.43	91.76	90.41	89.08	88.34	86.99	87.02

Speed(rpm)

(**a**) Efficiency test results applying SVPWM.

Torque(Nm) | %

	1,000	2,000	3,000	4,000	5,000	6,000	7,000	8,000	9,000	10,000
300	75.94	84.92	88.43							
280	76.11	85.05	88.72							
260	78.44	86.50	89.80							
240	80.48	87.73	90.73	91.26						
220	81.28	88.21	91.09	91.83						
200	82.62	89.03	91.68	92.56	91.37					
180	83.59	89.63	92.11	93.09	92.17					
160	83.92	89.77	92.19	93.19	92.3	91.12				
140	84.91	90.21	92.43	93.48	92.68	91.63	90.00			
120	85.61	90.53	92.60	93.70	92.95	91.99	90.52	89.58		
100	85.94	90.67	92.68	93.80	93.08	92.16	90.76	89.77		
80	86.26	90.68	92.50	93.59	92.95	92.01	90.48	89.54	88.64	88.07
60	86.64	90.70	92.29	93.36	92.80	91.83	90.15	89.27	88.32	87.58
40	87.02	90.71	92.08	93.12	92.65	91.65	89.82	88.99	87.99	87.08
20	87.14	90.35	92.04	92.76	92.43	91.44	89.66	88.65	87.70	86.71

Speed(rpm)

(**b**) Efficiency test results applying DPWM and RPWM.

Torque(Nm)

	1,000	2,000	3,000	4,000	5,000	6,000	7,000	8,000	9,000	10,000
300	7	7	4							
280	7	7	4							
260	3	7	7							
240	3	7	4	4						
220	3	7	4	4						
200	3	4	4	4	4					
180	3	4	4	4	4					
160	3	4	4	4	2	4				
140	3	4	4	4	2	6	4			
120	3	4	4	4	2	5	4	4		
100	3	4	4	4	2	6	4	2		
80	4	4	4	4	6	6	4	4	8	4
60	4	4	4	4	6	6	4	4	8	3
40	4	4	4	4	6	6	4	4	8	1
20	4	4	4	4	6	6	4	4	8	1

SVPWM	1
30°DPWM	2
60°DPWM	3
60°+30°DPWM	4
60°-30°DPWM	5
+120°DPWM	6
-120°DPWM	7
RPWM	8

Speed(rpm)

(**c**) Results of selection of maximum-efficiency PWM.

Torque(Nm) | RDPWM-SWPWM(%)

	1,000	2,000	3,000	4,000	5,000	6,000	7,000	8,000	9,000	10,000
300	1.52	1.04	0.54							
280	1.35	0.68	0.61							
260	1.56	0.66	0.37							
240	1.28	0.58	0.33	0.29						
220	1.18	0.55	0.31	0.34						
200	1.11	0.53	0.30	0.33	0.37					
180	1.06	0.53	0.30	0.32	0.46					
160	1.13	0.55	0.31	0.32	0.44	0.33				
140	1.33	0.62	0.34	0.30	0.36	0.37	0.35			
120	1.46	0.68	0.36	0.31	0.31	0.40	0.33	0.29		
100	1.53	0.70	0.37	0.31	0.28	0.41	0.33	0.18		
80	1.75	0.83	0.38	0.39	0.35	0.55	0.35	0.26	0.43	0.32
60	2.02	0.99	0.39	0.50	0.43	0.71	0.37	0.35	0.66	0.16
40	2.29	1.15	0.41	0.60	0.50	0.87	0.39	0.44	0.88	0.00
20	2.18	1.09	0.39	0.33	0.66	1.03	0.58	0.31	0.71	-0.31

Speed(rpm)

(**d**) Efficiency comparison results (D/RPWM−SVPWM).

Figure 12. Comparison of inverter and motor integrated system efficiency measurement results by speed and torque with SVPWM, RPWM, and DPWM applied.

3.2. NVH Measurements

Noise Frequency Analysis and Impact of PWM Techniques on NVH

The NVH experiment was designed to assess the noise and vibration effects of different PWM techniques. The motor was tested under 50% torque, while the speed was swept from 1000 rpm to 11,000 rpm. The analysis included eight types of PWM—SVPWM, DPWM (selected from Section 3.1.3 for maximum system efficiency), and RPWM—with SVPWM serving as the baseline for comparison. The setup for the NVH measurement adhered to IEEE standards, with microphones placed 1 m from the motor surface at three locations, Left Hand (LH), Right Hand (RH), and Top Side, as shown in Figure 13. For maximum power output conditions, powertrain performance typically takes priority over NVH characteristics. Therefore, NVH speed sweep tests are generally conducted at continuous power rather than maximum power. Accordingly, this NVH test was conducted at 50% continuous torque, aligning with industry standards for realistic NVH assessment.

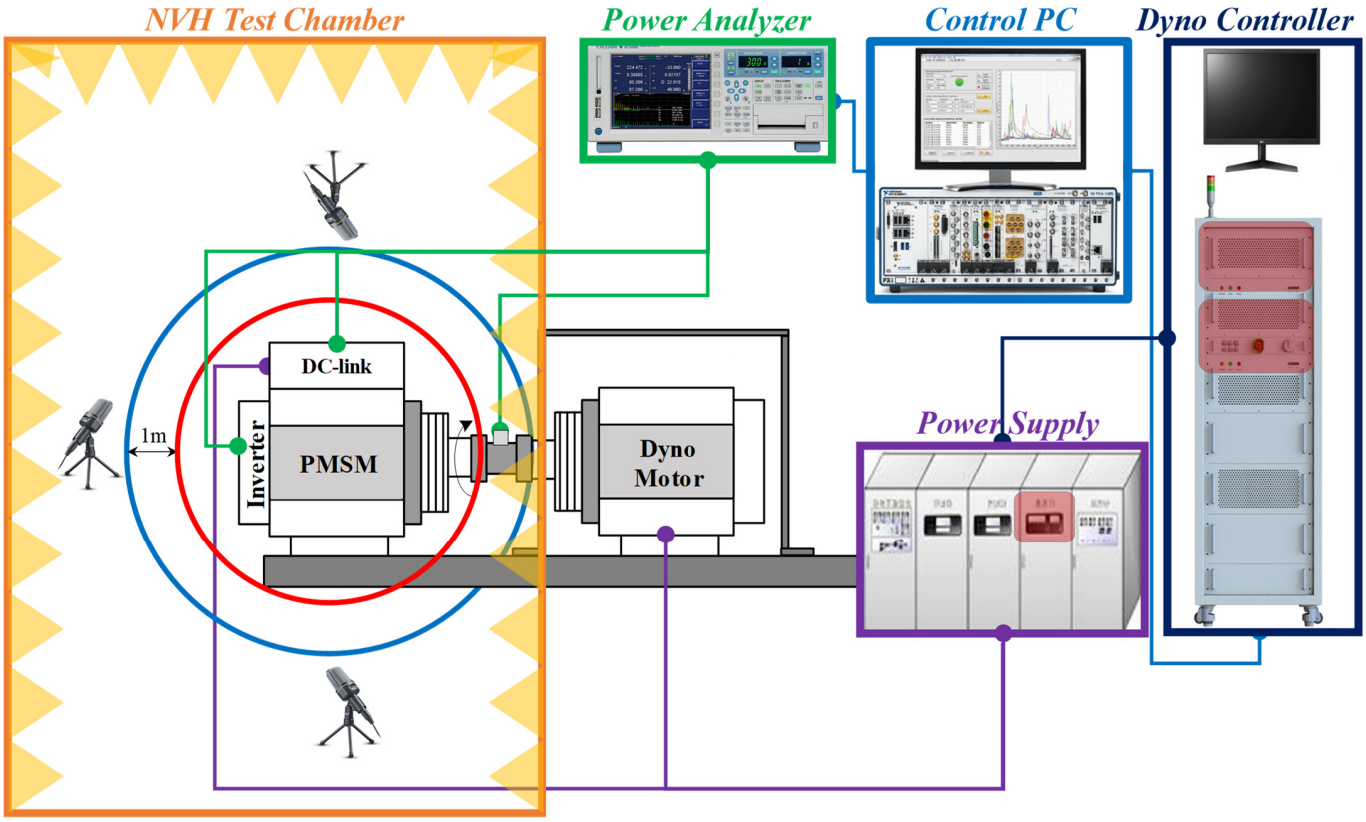

Figure 13. Environmental setup for NVH measurement.

The NVH Test Chamber (semi-anechoic chamber) technical specifications are as follows Table 3.

Table 3. The NVH Test Chamber technical specifications.

Parameters	Value	Unit
Chamber dimensions	8.5/8.5/4.5	M
Noise floor	20	dB(A)
Lower frequency limit	100	Hz

The Dyno(Dynamo) system technical specifications are as follows in Table 4.

Table 4. Dyno system technical specifications.

Parameters	Value	Unit
Maximum power	1000	kW
Maximum DC voltage	1200	V
Maximum current	1200	V
Speed range	−24,000~24,000	rpm
Maximum torque (nominal)	1200	Nm

As shown in Figure 14a, the NVH performances of RPWM and SVPWM are at similar levels, while SVPWM demonstrates superior NVH performance compared to DPWM. This finding aligns with the known characteristic of DPWM, which increases THD, thus leading to higher noise and vibration levels.

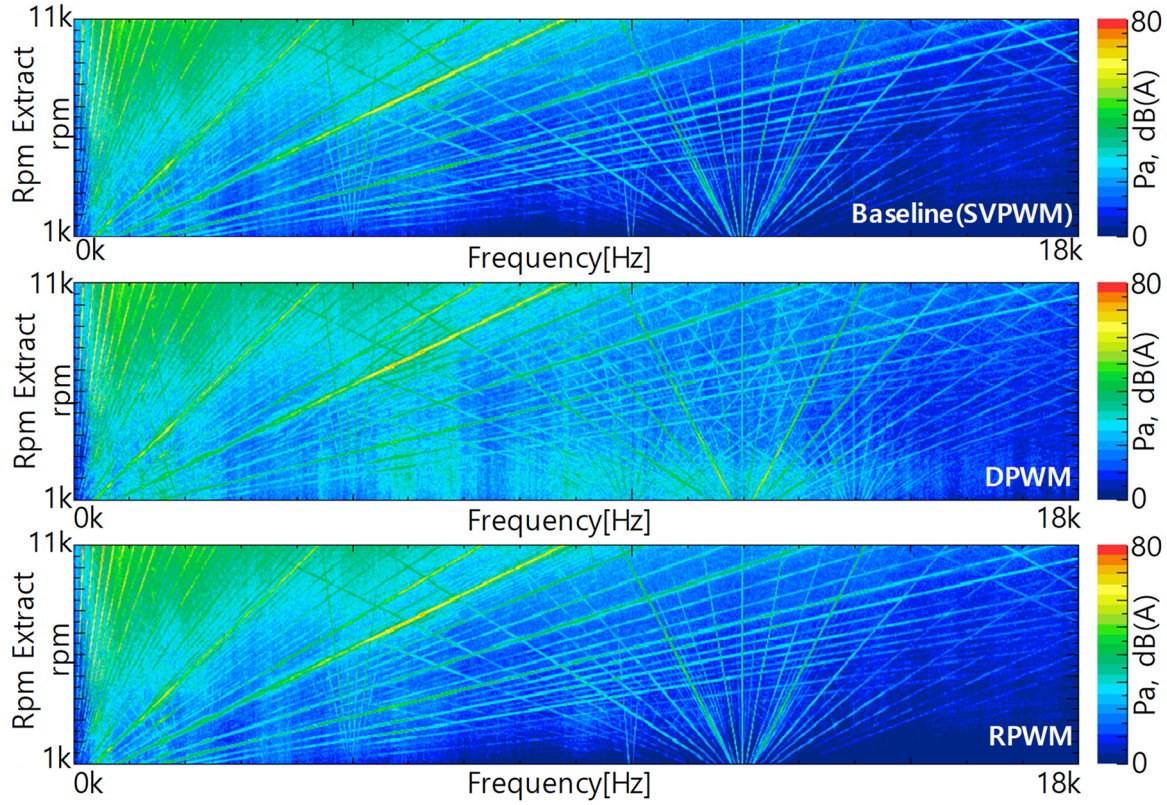

(**a**) NVH color map.

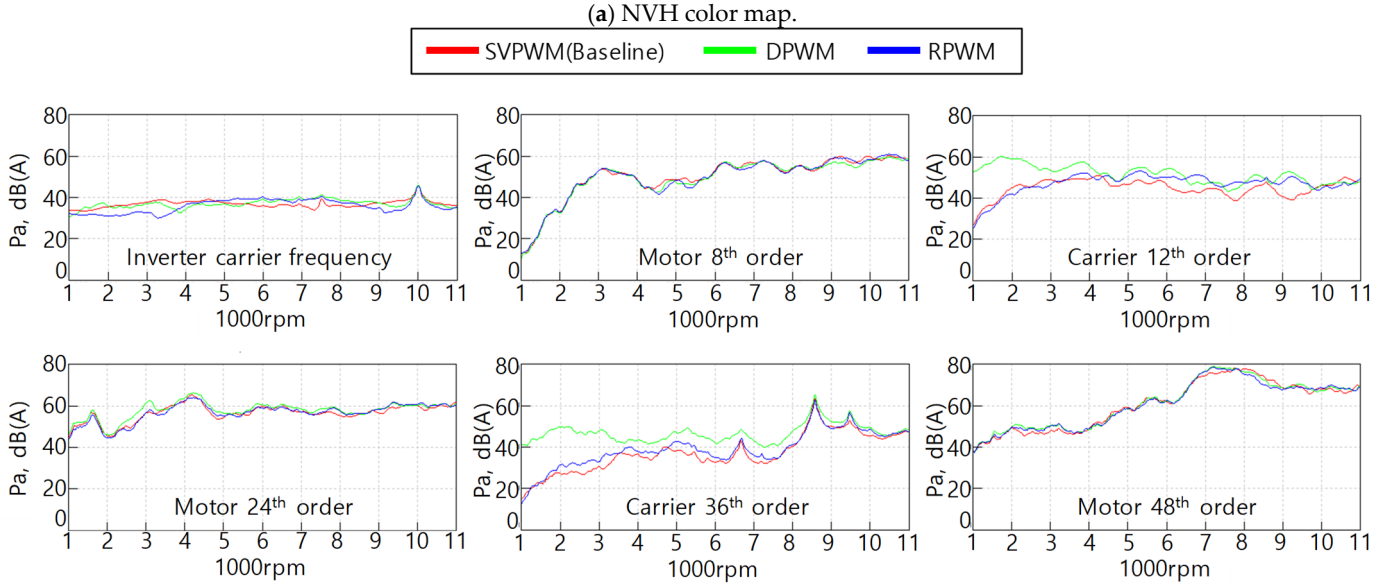

(**b**) NVH order tracking.

Figure 14. NVH experimental results for inverter and motor integrated system.

Figure 14b shows the NVH characteristics of SVPWM, DPWM, and RPWM by order. It highlights the variation in the size of the noise components generated by inverter switching depending on the PWM technique. Among the three PWM techniques, DPWM exhibited the poorest noise characteristics, while SVPWM and RPWM demonstrated similar levels of noise. In all test cases, DPWM was consistently shown to have inferior NVH performance compared to the baseline, regardless of the conditions.

4. Conclusions

This paper has presented a comparative analysis of the efficiency and NVH performance of various PWM techniques, including SVPWM, DPWM, and RPWM, for an electric vehicle inverter and motor system. The experimental results demonstrated that DPWM showed the highest efficiency, outperforming SVPWM by up to 2.23%. However, the efficiency benefits of DPWM were countered by its higher noise levels, as its increased THD negatively affected NVH performance. In contrast, SVPWM exhibited balanced performance with solid efficiency and NVH characteristics, making it a strong candidate for applications where noise is a key concern. RPWM, while showing similar NVH performance to SVPWM, offered the potential for noise reduction across a wider frequency band due to its ability to distribute harmonics.

The results also highlighted the impact of switching techniques on both system efficiency and noise. DPWM, while efficient, showed inferior NVH performance compared to SVPWM and RPWM, with significant noise generation from inverter switching components. This confirms the trade-off between efficiency and NVH performance, particularly when choosing switching techniques for practical applications.

In the case of RPWM, there is a possibility of NVH performance changing depending on the gain factor, and additional experiments are needed while adjusting the factor. Further investigations into the optimal settings for RPWM could improve its NVH performance without sacrificing efficiency, making it a promising technique for future research.

Funding: This research received no external funding.

Data Availability Statement: The original contributions presented in this study are included in the article; further inquiries can be directed to the corresponding author.

Conflicts of Interest: The author declares no conflicts of interest.

References

1. Ehsani, M.; Gao, Y.; Longo, S.; Ebrahimi, K. *Modern Electric, Hybrid Electric, and Fuel Cell Vehicles*; CRC Press: Boca Raton, FL, USA, 2018.
2. Zhang, X.; Mi, C.C. *Vehicle Power Management: Modeling, Control and Optimization*; Springer: London, UK, 2011.
3. Ehsani, M.; Gao, Y.; Emadi, A. *Modern Electric, Hybrid Electric, and Fuel Cell Vehicles: Fundamentals, Theory, and Design*, 2nd ed.; CRC Press: Boca Raton, FL, USA, 2009.
4. Rodríguez, J.; Lai, J.S.; Peng, F.Z. Multilevel inverters: A survey of topologies, controls, and applications. *IEEE Trans. Ind. Electron.* **2002**, *49*, 724–738. [CrossRef]
5. Bose, B.K. *Modern Power Electronics and AC Drives*; Prentice Hall: Hoboken, NJ, USA, 2002.
6. Holmes, D.G.; Lipo, T.A. *Pulse Width Modulation for Power Converters: Principles and Practice*; John Wiley & Sons: Hoboken, NJ, USA, 2003.
7. Hava, A.M.; Kerkman, R.J.; Lipo, T.A. Simple analytical and graphical methods for carrier-based PWM-VSI drives. *IEEE Trans. Power Electron.* **1999**, *14*, 49–61. [CrossRef]
8. Wu, B. *High-Power Converters and AC Drives*; John Wiley & Sons: Hoboken, NJ, USA, 2006.
9. Kazmierkowski, M.P.; Krishnan, R.; Blaabjerg, F. *Control in Power Electronics: Selected Problems*; Academic Press: New York, NY, USA, 2002.
10. Habetler, T.G.; Divan, D.M. Acoustic noise reduction in sinusoidal PWM drives using a randomly modulated carrier. *IEEE Trans. Power Electron.* **1991**, *6*, 356–363. [CrossRef]
11. Franquelo, L.G.; Rodriguez, J.; Leon, J.I.; Kouro, S.; Portillo, R.; Prats, M.A.M. The age of multilevel converters arrives. *IEEE Ind. Electron. Mag.* **2008**, *2*, 28–39. [CrossRef]
12. Kouro, S.; Malinowski, M.; Gopakumar, K.; Pou, J.; Franquelo, L.G.; Wu, B.; Rodriguez, J.; Pérez, M.A.; Leon, J.I. Recent Advances and Industrial Applications of Multilevel Converters. *IEEE Trans. Ind. Electron.* **2010**, *57*, 2553–2580. [CrossRef]
13. Holtz, J. Pulsewidth Modulation-A Survey. *IEEE Trans. Ind. Electron.* **1992**, *39*, 410–420. [CrossRef]
14. van der Broeck, H.W.; Skudelny, H.-C.; Stanke, G.V. Analysis and realization of a pulsewidth modulator based on voltage space vectors. *IEEE Trans. Ind. Appl.* **1988**, *24*, 142–150. [CrossRef]
15. Kazmierkowski, M.P.; Franquelo, L.G.; Rodriguez, J.; Perez, M.A.; Leon, J.I. High-Performance Motor Drives. *IEEE Ind. Electron. Mag.* **2011**, *5*, 6–26. [CrossRef]
16. Malinowski, M.; Gopakumar, K.; Rodriguez, J.; Perez, M.A. A Survey on Cascaded Multilevel Inverters. *IEEE Trans. Ind. Electron.* **2010**, *57*, 2197–2206. [CrossRef]

17. Zhou, K.; Wang, D. Relationship between space-vector modulation and three-phase carrier-based PWM: A comprehensive analysis. *IEEE Trans. Ind. Electron.* **2002**, *49*, 186–196. [CrossRef]
18. Iqbal, A.; Levi, E.; Jones, M.; Vukosavic, S.N. Generalised sinusoidal PWM with harmonic injection for multi-phase VSIs. In Proceedings of the 37th IEEE Power Electronics Specialists Conference, Jeju, Republic of Korea, 18–22 June 2006; pp. 1–7.
19. Narayanan, G.; Ranganathan, V.T. Two novel synchronized bus-clamping PWM strategies based on space vector approach for high power drives. *IEEE Trans. Power Electron.* **2002**, *17*, 84–93. [CrossRef]
20. Ojo, O. The generalized discontinuous PWM scheme for three-phase voltage source inverters. *IEEE Trans. Ind. Electron.* **2004**, *51*, 1280–1289. [CrossRef]
21. Trzynadlowski, A.M.; Blaabjerg, F.; Pedersen, J.K.; Kirlin, R.L.; Legowski, S. Random pulse width modulation techniques for converter-fed drive systems-a review. *IEEE Trans. Ind. Appl.* **1994**, *30*, 1166–1175. [CrossRef]
22. Lai, Y.-S.; Chang, Y.-T. Design and implementation of vector-controlled SPWM inverter using a DSP and FPGA. *IEEE Trans. Ind. Electron.* **2003**, *50*, 116–127.
23. Bech, M.M.; Pedersen, J.K.; Blaabjerg, F. Random modulation techniques with fixed switching frequency for three-phase power converters. *IEEE Trans. Power Electron.* **2000**, *15*, 753–761. [CrossRef]